

Identification of Homologous Biologically Active Sites on the N-Terminal Domain of Laminin Alpha Chains[†]

Motoyoshi Nomizu,^{*,§} Fumiharu Yokoyama,[§] Nobuharu Suzuki,[§] Ikuko Okazaki,[§] Norio Nishi,[§] M. Lourdes Ponce,[‡] Hynda K. Kleinman,[‡] Yoko Yamamoto,[#] Shinsaku Nakagawa,[#] and Tadanori Mayumi[#]

Graduate School of Environmental Earth Science, Hokkaido University, Sapporo 060-0810, Japan, Craniofacial Developmental Biology and Regeneration Branch, National Institute of Dental and Craniofacial Research, National Institutes of Health, Bethesda, Maryland 20892, USA, Graduate School of Pharmaceutical Sciences, Osaka University, Osaka 565-0871, Japan

Received July 24, 2001; Revised Manuscript Received September 24, 2001

ABSTRACT: Laminin, a multifunctional glycoprotein of the basement membrane, consists of three different subunits, α , β , and γ chains. To date, five different α chains have been identified. N-terminal domain VI in the $\alpha 1$ chain has various biological activities. Here we screened biologically active sequences on domain VI of the laminin $\alpha 2$, $\alpha 3$, and $\alpha 5$ chains using a large number of overlapping peptides. HT-1080 human fibrosarcoma cell attachment to the peptides was evaluated using peptide-coated plastic plates and peptide-conjugated Sepharose beads. We identified four cell adhesive sequences from laminin $\alpha 2$ chain domain VI, two sequences from the $\alpha 3$ chain, and two sequences from the laminin $\alpha 5$ chain. Sequences homologous to A13 (RQVFQVAYIIKA, $\alpha 1$ chain 121–133) on all the α chains (FQIAYVIVKA, $\alpha 2$ chain 130–139; GQLFHVAYILIKF, $\alpha 3$ chain 96–108; FHVAYVLIKA, $\alpha 5$ chain 74–83) showed strong cell attachment activity. A5–16 (LENGEIVVSLVNGR, $\alpha 5$ chain 147–160) showed the strongest cell attachment activity in the plate assay, and the homologous peptide in the $\alpha 3$ chain promoted similar strong cell attachment activity. A5–16 and its homologous peptide in the $\alpha 2$ chain promoted moderate cell attachment, while the homologous peptide to A5–16 in the $\alpha 1$ chain did not show activity. A2–7 (SPSIKNGVEYHYV, $\alpha 2$ chain 108–120) showed cell attachment activity only in the plate assay, but homologous sequences in the $\alpha 1$, $\alpha 3$, and $\alpha 5$ chains did not promote activity. A2–7 promoted endothelial cell sprouting from aortic rings in vitro and melanoma colonization to murine lungs in vivo. However, none of the homologous peptides of A2–7 promoted experimental pulmonary metastasis by B16–BL6 melanoma cells. These results indicate that there are chain-specific active sites in domain VI of the laminin α chains, some of which contain conserved activities.

Laminin, a multifunctional glycoprotein of the basement membrane, consists of three different subunits, α , β , and γ chains (1). So far, five α , three β , and three γ chains have been identified, and at least 15 isoforms are formed by various combinations of each subunit (2–4). Laminin has diverse biological activities including promotion of cell adhesion, migration, neurite outgrowth, tumor metastasis, and angiogenesis (1). More than 20 receptors have been reported for the laminin-1 molecule (5). Several active sites on laminin-1 have been identified using proteolytic fragments, recombinant proteins, and synthetic peptides (6, 7). We have screened cell adhesive sequences on laminin-1 using 673 overlapping synthetic peptides covering the entire protein (8–11). Most of the active peptides were localized in the

globular domains and found to play a critical role in binding to cell surface receptors in a peptide- and cell type-specific manner (12, 13). Several peptides were found to interact with both integrins and syndecan (14–16). Some of the peptides promoted neurite outgrowth, angiogenesis, and tumor metastasis (17–20).

Domain VI of the α chain, one of the globular domains in laminin, is located on the N-terminus and is important for many activities of laminin, such as cell adhesion, neurite outgrowth, perlecan binding, and self-assembly (21–23). Domain VI of laminin $\alpha 1$, $\alpha 2$, and $\alpha 5$ chains interacts with $\alpha 1\beta 1$, $\alpha 2\beta 1$, and $\alpha 3\beta 1$ integrins. This domain also binds to heparin and to heparan sulfate. Previously, we identified several cell binding sites in domain VI of the laminin $\alpha 1$ chain (10). A13 (RQVFQVAYIIKA), derived from laminin $\alpha 1$ chain domain VI, showed the strongest cell attachment activity (10). The A13 peptide promoted integrin-mediated cell adhesion, migration, angiogenesis, and tumor metastasis (10, 16, 19, 24). These results suggest that domain VI plays a critical role in some of the biological functions of laminin.

Domain VI is contained within the $\alpha 1$, $\alpha 2$, $\alpha 3$, and $\alpha 5$ chains (2–4). The $\alpha 2$ chain is localized in the basement membranes of skeletal muscle and peripheral nerve (25), while the $\alpha 3$ chain is mainly localized in epithelial tissues

[†] This work was supported in part by the Grants-in-Aid for Scientific Research from Ministry of Education, Science, Sports, and Culture of Japan (Nos. 11470480, 11139201, and 12215002) and by the Research Foundation for Pharmaceutical Sciences.

^{*} To whom correspondence should be addressed: Motoyoshi Nomizu, Ph.D. Graduate School of Environmental Earth Science, Hokkaido University, Kita 10 Nishi 5, Kita-ku, Sapporo 060–0810, Japan. Phone/Fax: 81-11-706-2254. E-mail: nomizu@ees.hokudai.ac.jp.

[§] Hokkaido University.

[‡] National Institutes of Health.

[#] Osaka University.

(3, 26). The $\alpha 5$ chain is more widely distributed, and changes in its levels are associated with diverse pathologies, such as defective glomerulogenesis, sickle red blood cell (RBC) adhesion, and diabetic retinopathy (27–29).

In this paper, we describe the systematic screening for biologically active sequences in domain VI of mouse laminin $\alpha 2$, $\alpha 3$, and $\alpha 5$ chains using a large set of overlapping peptides. As the first stage of screening, we examined the cell attachment activity of 74 different peptides using peptide-conjugated Sepharose beads and peptide-coated plates. Eight active sequences were identified. Several additional biological activities, including angiogenesis and tumor metastasis, were also evaluated using the most active synthetic peptides.

MATERIALS AND METHODS

Synthetic Peptides. All peptides were synthesized manually using the 9-fluorenylmethoxycarbonyl (Fmoc) based solid-phase strategy and prepared in the C-terminal amide form as previously described (10). Amino acid derivatives and resins were purchased from Watanabe Chemical, Hiroshima, Japan, and Novabiochem, La Jolla, CA. The respective amino acids were condensed manually in a stepwise manner using 4-(2',4'-dimethoxyphenyl-Fmoc-aminomethyl)-phenoxy resin. Dimethylformamide was used during the synthesis as a solvent. For condensation, diisopropylcarbodiimide/*N*-hydroxybenzotriazole was employed, and for deprotection of *N*^α-Fmoc groups, 20% piperidine in *N*-methyl pyrrolidone was employed. The following side chain protecting groups were used: Asn, Gln, and His, trityl; Asp, Glu, Ser, Thr, and Tyr, *tert*-butyl; Arg, 2,2,5,7,8-pentamethylchroman-6-sulfonyl; and Lys, *tert*-butoxycarbonyl. Resulting protected peptide resins were deprotected and cleaved from the resin using a trifluoroacetic acid-thioanisole-*m*-cresol-ethanedithiol-H₂O (80:5:5:5:5, v/v) at 20 °C for 2 h. Resulting crude peptides were precipitated and washed with ethyl ether, then purified by reverse-phase high performance liquid chromatography (using a Vydac 5C18 column and a gradient of water/acetonitrile containing 0.1% trifluoroacetic acid). Purity of the peptides was confirmed by analytical high performance liquid chromatography. Identity of the peptides was confirmed by a Sciex API IIIIE triple quadrupole ion spray mass spectrometer. Five peptides showed low solubility in aqueous solutions and could not be purified by reverse-phase high performance liquid chromatography.

Preparation of Peptide-Conjugated Sepharose Beads. The 73 soluble peptides (one was not soluble) from domain VI of the $\alpha 2$, $\alpha 3$, and $\alpha 5$ chains were coupled to cyanogen bromide (CNBr)-activated Sepharose 4B (Pharmacia Biotech AB, Uppsala, Sweden) as described previously (30). The peptide solutions (0.2 mL, 1 mg/mL in Milli-Q H₂O) were mixed with 30 mg of the activated Sepharose beads. Ethanamine-coupled beads were prepared as a control. The amounts of coupled peptide were determined by amino acid analysis (10–20 μ mol of peptides/g of Sepharose bead) (30).

Cells and Culture. HT-1080 human fibrosarcoma cells (31) were maintained in Dulbecco's modified Eagle's medium (DMEM, Life Technologies, Rockville, MD) containing 10% fetal bovine serum (FBS, Life Technologies), 100 units/mL penicillin, and 100 μ g/mL streptomycin (Life Technologies). B16–BL6 mouse melanoma cells were maintained in Eagle's minimal-essential medium (MEM) containing 5% FBS, 100 units/mL penicillin, and 100 μ g/mL streptomycin.

Cell Attachment Assay Using Peptide-Conjugated Beads. Cell attachment to peptide-Sepharose or to polystyrene beads was assayed in 96-well dishes. HT-1080 and B16–BL6 cells were detached by 0.02% EDTA in phosphate-buffered saline (Versene, Life Technologies), and then washed with DMEM containing 0.1% bovine serum albumin (BSA, Sigma). The cells (10 000/100 μ L of DMEM containing 0.1% BSA) were incubated with 20 μ L of the bead solution at 37 °C for 1 h in 5% CO₂. The cells that attached to the beads were stained with a 0.2% crystal violet aqueous solution in 20% methanol for 10 min and analyzed under the microscope. Cell attachment was quantitated in triplicate and evaluated on the following subjective scale: ++, adhesion comparable to that of A13; +, adhesion weaker than that of A13; –, no adhesion.

Cell Attachment Assay Using Synthetic Peptides. Cell attachment to peptide-coated plates was assayed in 96-well plates (Nunc Inc., Naperville, IL). Plates were coated with various amounts of peptide in 50 μ L of Milli-Q H₂O by drying overnight. The wells were blocked by addition of 100 μ L of 3% BSA in DMEM for 1 h, then washed twice with DMEM containing 0.1% BSA. Cells, detached by Versene and resuspended in DMEM containing 0.1% BSA, were added (30 000/100 μ L) to each well and incubated at 37 °C for 30 min in 5% CO₂. The attached cells were stained with 0.2% crystal violet aqueous solution in 20% methanol for 10 min. After washing off the unattached cells, 200 μ L of 1% SDS was used to solubilize the cellular proteins, and the optical density at 570 nm was measured in a model 550 Microplate reader (Bio-Rad Laboratories, Hercules, CA).

In heparin and EDTA inhibition experiments, 5 mM EDTA was added to the HT-1080 cell suspensions 10 min before plating the cells. In heparin inhibition experiments, 10 μ g/mL heparin was added to both the wells and HT-1080 cell suspensions 10 min before plating the cells. After a 30 min incubation, the attached cells were measured as described above. All assays were carried out in triplicate, and each experiment was repeated at least three times.

Aortic Ring Assay. The aortic ring assay was performed as described previously (19). Aortas were harvested from 6-wk-old Sprague–Dawley rats and immediately placed in RPMI 1640 (Life Technologies). Fatty tissues were removed by gentle scraping, and the aortas were cut into thin rings with a scalpel (32). Since the ends of the aortas were held by forceps during the cleaning and cutting and may have been damaged, they were discarded. Forty-eight-well plates were coated with 110 μ L of Matrigel, and the rings were placed on the Matrigel and sealed in place with an overlay of 40 μ L of Matrigel. Various amounts (0.4, 0.2, or 0.1 mg) of each peptide were added to the wells in a final volume of 200 μ L of human endothelial serum-free media (Life Technologies). As controls, medium alone and medium containing 200 μ g/mL of endothelial cell growth supplement (ECGS) (Collaborative Research, Bedford, MA) were assayed. Additional peptide was added on day 4, and the assay was fixed and stained with Diff-Quik on days 5–7. Each data point was assayed in quadruplicate (triplicates for the dose response), and each experiment was repeated at least three times. A blinded observer scored outgrowth by comparing responses with media alone (background levels) to that observed with the peptides and with ECGS (positive control). Results were scored with the following scale ++,



FIGURE 1: Sequences and peptides from the domain VI of laminin $\alpha 2$, $\alpha 3$, and $\alpha 5$ chains. Sequences were derived from mouse laminin $\alpha 2$, $\alpha 3$, and $\alpha 5$ chains (3, 39, 40). Locations of peptides are indicated by arrows. Active peptide sequences in peptide-coated plate and/or peptide-conjugated bead assays are shown by bold arrows.

sprouting comparable to ECGS; +, significant sprouting but lower than positive control; and –, low levels of sprouting comparable to background levels.

In Vivo Experimental Pulmonary Metastasis Assay. In vivo experimental pulmonary metastasis assays were carried out as described previously (33). 100 μ L of B16–BL6 cells (1 500 000 cells/mL in MEM containing 0.1% BSA) were injected into the tail vein of C57BL6J mice (6 weeks old, male). Then immediately 100 μ L of peptide solution (1 mg/mL in MEM containing 0.1% BSA) were injected into the tail vein. The mice were sacrificed 15 days after injection. The lungs were removed, and the number of visible colonies on the lung surface was counted. Each peptide was assayed in five mice, and the active peptides were tested a minimum of two times.

RESULTS

Cell Attachment Activity of Synthetic Peptides Derived from Domain VI of the Laminin $\alpha 2$, $\alpha 3$, and $\alpha 5$ Chains. We prepared 74 peptides from laminin domain VI of $\alpha 2$, $\alpha 3$, and $\alpha 5$ chains for screening of cell binding sequences (Figure 1). These peptides were dissolved in Milli-Q water except for A2–9, which was insoluble. As a positive control, A13 (RQVFQVAYIIKA), which has the strongest cell attachment activity in the $\alpha 1$ chain domain VI, was used (10). We used HT-1080 human fibrosarcoma and B16–BL6 mouse melanoma cells for evaluating cell attachment activity. In $\alpha 2$ chain domain VI, A2–20 (LEFTSARYIRLR) showed strong activity comparable to that of A13 (Figure 2). Two peptides (A2–7 and A2–8) showed moderate cell attachment activity. None of the other $\alpha 2$ chain peptides was active. In $\alpha 3$ chain domain VI, A3–10 (GQLFHVAYILIKF) showed strong cell attachment activity comparable to that of A13

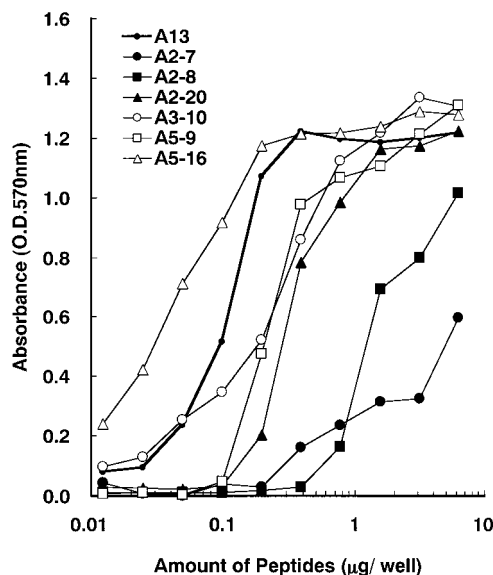


FIGURE 2: Attachment of HT-1080 cells to peptide-coated plates. 96-well plates were coated with various amounts of peptides. HT-1080 cells were added, and after 1 h the number of attached cells was assessed by crystal violet staining. Data are expressed as the mean of triplicate results. Triplicate experiments gave similar results.

and had a similar dose-dependent curve to that of A13 (Figure 2). None of the other $\alpha 3$ chain peptides was active. In $\alpha 5$ chain domain VI, A5–9 (AYVLIKFANSRR) and A5–16 (LENGEIVVSLVNGR) showed strong cell attachment activity comparable to that of A13 and had a similar dose-dependent curve to that of A13 (Figure 2). In contrast, none of the $\alpha 5$ other peptides showed cell adhesion to the plates.

We next evaluated cell attachment activity of all the peptides after coupling to beads using HT-1080 cells.

Table 1: Synthetic Laminin α Chain Domain VI Peptides and their Cell Attachment Activities

pept	sequence	cell attachment activity				
		HT-1080		B16-BL6	aortic sprout ^c	promot of lung coloniz ^d
		plate ^a	bead ^b	plate ^a		
A2-7	SPSIKNGVEYHYV	+	—	+	+	+
A2-8	YHYVTITLQLQ	+	—	+	+(weak)	+
A2-20	LEFTSARYIRLR	++	+	++	—	—
A2-21	IRLRFQIRITLN	—	++	—	—	—
A3-10	GQLFHVAYILIKF	++	++	++	+	+
A3-22	TKATNIRLRFLR	—	+	—	+	—
A5-9	AYVLKIFANSR	++	+	++	—	—
A5-16	LENGEIVVSLVNGR	++	—	++	—	—
A13	RQVFQVAYIIKA	++	++	++	++	+

^a For cell attachment assays, various amounts of peptides were coated on the wells as described in Material and Methods. In all cases, the biological activities were quantitated, and peptide activities were evaluated relative to the activity observed with A13 as shown in Figure 2. Cell attachment was evaluated on the following subjective scale: ++, adhesion comparable to that of A13; +, adhesion weaker than that of A13; —, no adhesion. Triplicate experiments gave similar results. ^b Cell attachment activity on peptide-conjugated Sepharose beads. Cell attachment was evaluated on the following subjective scale: ++, adhesion comparable to that of A13; +, adhesion weaker than that of A13; —, no adhesion. Triplicate experiments gave similar results. ^c Endothelial cell sprouting from aortic segments in the presence of peptides was tested. Results were scored with the following scale: ++, sprouting comparable to ECGS; +, significant sprouting but lower than positive control; —, low levels of sprouting background levels. ^d B16-BL6 cells and peptides were separately injected via the tail veins of C57BL6/N mice. The lungs were removed after 15 days, and the number of the colonies on the surface of the lung was counted. Promotion of lung colonization was shown: +, significantly increased number of lung colonies similar to that of A13; —, not changed.

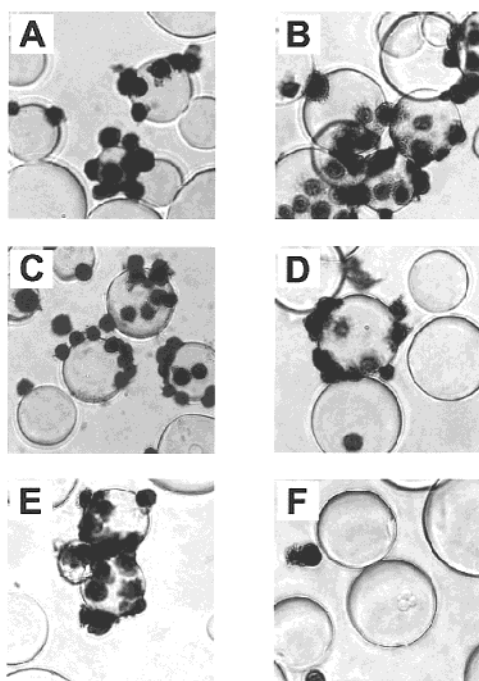


FIGURE 3: Adhesion of HT-1080 cells on peptide-conjugated Sepharose beads. HT-1080 human fibrosarcoma cells were allowed to attach to peptide-conjugated Sepharose beads for 1 h and were then stained with crystal violet. (A) A2-20; (B) A2-21; (C) A3-22; (D) A5-9; (E) A13; (F) ethanolamine. Original magnification 200 \times .

Seventy-three soluble peptides (except insoluble peptide A2-9) were coupled to CNBr-activated Sepharose beads. A13-conjugated beads were used as a positive control. Ethanolamine-conjugated beads were also prepared as a negative control. HT-1080 cells attached and spread on A13-conjugated Sepharose beads, while ethanolamine beads did not show cell attachment activity (Figure 3). In α 2 chain domain VI, A2-21-conjugated beads showed strong cell attachment and spreading activity comparable to that of A13 (Figure 3B, E). A2-20-conjugated beads showed moderate cell attachment. In α 3 chain domain VI, A3-10-conjugated beads showed strong cell attachment activity comparable to

that of A13-conjugated beads (Table 1). A3-22-conjugated beads showed moderate cell attachment activity (Figure 3C). In α 5 chain domain VI, only A5-9-conjugated beads showed moderate cell attachment activity. A5-16, which was the most active in the plate assay, did not support cell attachment to the beads. The remainder of the peptide beads did not have significant cell attachment activity. On the basis of the two cell attachment assays, we found eight potentially active peptides (Table 1).

Effects of EDTA and Heparin on Cell Attachment. The effects of EDTA on HT-1080 cell attachment to peptide-coated plates were examined to determine the role of cations using the seven peptides that were active in the plate assays including A13 (Figure 4). Cell attachment to laminin-1 was inhibited by 5 mM EDTA as shown previously (10). Cell attachment of A2-8 was inhibited by 5 mM EDTA. While EDTA did not affect cell attachment to the rest of the active peptides. These results suggest that HT-1080 cells attach to the A2-8 peptide in a cation-dependent manner.

Next, we tested the effects of heparin on HT-1080 cell attachment to peptide-coated plates using the seven peptides that were active when coated on the plates (Figure 4). Cell attachment to laminin-1 was not inhibited by 10 μ g/mL heparin, whereas attachment to A13 was inhibited by 10 μ g/mL heparin as shown previously (10). Cell attachment to all of the peptides was inhibited in the presence of 10 μ g/mL heparin except cell attachment to A2-8, which was not affected by heparin. These data suggest that negatively charged molecules may function as cellular surface ligands for the laminin α chain active sequences (A13, A2-7, A2-20, A3-10, A5-9, and A5-16).

Endothelial Sprouting. Next, we focused on eight peptides (Table 1) that showed strong cell attachment activity in the plate and/or bead assays. We tested for endothelial sprouting activity using rat aortic rings (Figure 5). A13 stimulated vessel sprouting as described previously (19). A2-7, A3-10, and A3-22 also stimulated vessel sprouting, and A2-8 showed weak activity; whereas, the remaining cell adhesive peptides were not active in this assay (Table 1).

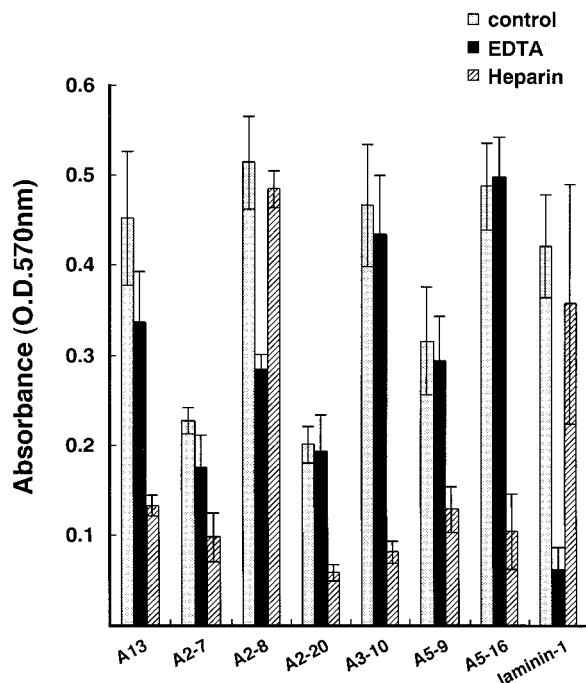


FIGURE 4: Inhibition of HT-1080 cell attachment to peptides by EDTA and by heparin. Round-bottom 96-well plates were coated with 2 μ g of peptide/well. 5 mM EDTA or 10 μ g/mL heparin were added to cell suspensions and incubated for 10 min. Then cells were added onto the plates. After a 30 min incubation, the attached cells were assessed by crystal violet staining. Each value represents the mean of five separate determinations \pm SD. Duplicate experiments gave similar results.

In Vivo Experimental Pulmonary Metastasis Assay. The effect of the eight cell adhesive peptides on experimental pulmonary metastasis by B16–BL6 cells in vivo was tested (Table 1). B16–BL6 mouse melanoma cells (150 000/mouse) were intravenously injected via the tail vein into C57BL/6J mice, and then peptides (0.1 mg/mouse) were immediately administered. After 15 days, the number of the metastatic colonies on the surface of the lungs was counted. Control cells (PBS injected without peptide) formed an average of 297 colonies per mouse lung (Table 1). A13 (a positive control) significantly promoted lung colonization as described previously (24). A2–7, A2–8, and A3–10 also significantly promoted lung colonization (Table 1). In contrast, the rest of the peptides did not significantly affect experimental metastasis.

Since the A2–7 peptide was active in promoting endothelial sprouting in vitro and in promoting metastasis in vivo, we studied the homologous peptides on the α 1, α 3, and α 5 chains for their activity (Table 2). Although these peptides did not promote B16–BL6 cell attachment, α 1(A2–7) and A5–6 were tested for their activity in the experimental pulmonary metastasis assay (Table 2). α 1(A2–7) and A5–6 did not promote experimental pulmonary metastasis (Table 2). Scrambled peptides of A2–7, A2–7S, and A2–7T also did not affect experimental pulmonary metastasis.

Since A13, A3–10, and A5–16 have the strongest cell attachment activity, we focused on these sequences and their homologues (Figure 6). We prepared the homologous peptides of A13 and A5–16 in truncated forms. A13b and A5–16a, which are truncated peptides of A13 and A5–16, were used because they bound to HT-1080 cells with activity comparable to the original peptides (Table 3). We evaluated

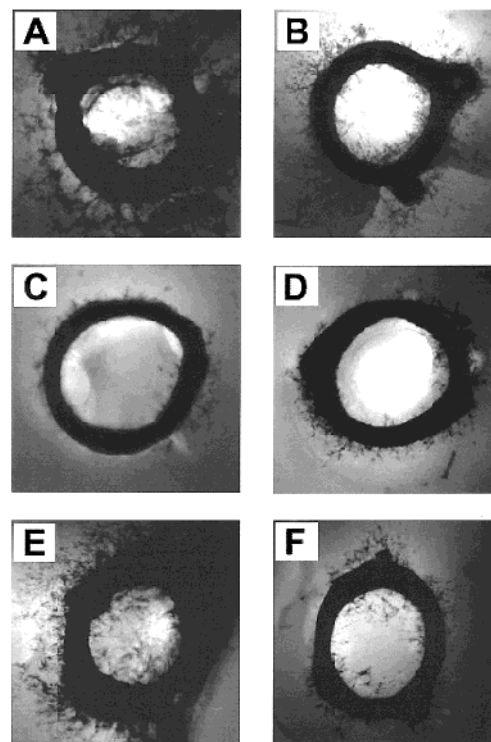


FIGURE 5: Stimulation of endothelial sprouting from aortic rings observed with 0.2 mg/mL of laminin peptides: (A) A13; (B) A2–7; (C) A5–9; (D) A5–16; (E) Matrigel with 200 μ g/mL ECGS (positive control); (F) Matrigel alone (negative control). Original magnification 5 \times .

Table 2: Effect of A2–7 and Related Peptides on Lung Colonization by B16–BL6 Melanoma Cell.

peptide	sequence	B16–BL6 cell attachment ^a	no. of lung colonies ^b
A2–7	SPSIKNGVEYHYV (α 2 chain 108–120)	+	369.0 \pm 10.9
α 1(A2–7)	SPSIQNGREYHWV (α 1 chain 102–114)	–	225.3 \pm 23.9
A3–8	SPPLSSGTQYNQVN (α 3 chain 77–90)	–	ND
A5–6	SPPLSRGLEYNEV (α 5 chain 52–64)	–	227.0 \pm 24.8
A2–7S	GYSIEPKSYHNVV (scrambled A2–7)	–	186.7 \pm 33.0
A2–7T	ISGEVPNYVHKYS (scrambled A2–7)	–	205.6 \pm 17.5
none			198.4 \pm 28.4

^a For cell attachment assays, various amounts of peptides were coated on the wells as described in Material and Methods. In all cases, the biological activities were quantitated and peptide activities were evaluated relative to the activity observed with A2–7 as shown in Figure 2. Cell attachment was evaluated on the following subjective scale: +, adhesion comparable to that of A2–7; –, no adhesion. Triplicate experiments gave similar results. ^b Each mouse was injected with 100 000 B16–BL6 cells via the tail vein and the peptide (0.1 mg/mouse) was immediately administered by tail vein. The number of colonies on the lungs was counted 15 days later. Number of lung colonies: mean \pm standard error. The experiment was repeated with similar results.

HT-1080 cell attachment activity in the peptide-coated plastic plate assay (Table 3). The homologous peptides for A13b in the α 2 and α 5 chains, α 2(A13b) and α 5(A13b), showed strong cell attachment activity comparable to that of A13b. This demonstrated complete conservation of the A13 activity

FIGURE 6: Alignment of amino acid sequences of the laminin α chain domain VI. Data are from $\alpha 1$: mouse laminin $\alpha 1$ chain (41); $\alpha 2$: mouse laminin $\alpha 2$ chain (39); $\alpha 3$: mouse laminin $\alpha 3$ chain (3); and $\alpha 5$: mouse laminin $\alpha 5$ chain (40) chains. Active sequences are boxed in black.

peptide	sequence	cell attachment plate ^a
A13	RQVFQVAYIIKA (α1 chain 121–133)	++
A13b	FQVAYIIKA (α1 chain 124–133)	++
α2(A13b)	FQIAYVIVKA (α2 chain 130–139)	++
A3–10	GQLFHVAYILIKF (α3 chain 96–108)	++
α5(A13b)	FHVAYVLIKA (α5 chain 74–83)	++
A5–16	LENGEIVVSLVNGR (α5 chain 147–160)	++
A5–16a	NGEIVVSLVNGR (α5 chain 149–160)	++
α1(A5–16a)	HGEIHTSLINGR (α1 chain 201–212)	–
α2(A5–16a)	NGEIHISLINGR (α2 chain 207–218)	+
α3(A5–16a)	NGEIVVSLINGR (α3 chain 174–185)	++
A5–16S	ILENVGEVNGRLVS (scrambled A5–16)	–

in all of the chains. In contrast, the homologues of the highly active A5-16 were not as active. The $\alpha 3$ (A5-16a) peptides, A5-16a homologous peptides in the $\alpha 3$ chain, showed activity in the plate assay comparable that of A5-16a, while $\alpha 2$ (A5-16a) showed moderate cell attachment activity. However, $\alpha 1$ (A5-16a) and the scrambled peptide (A5-16S) showed no activity in this assay. These results suggest that there are chain- and/or site-specific active sites.

Cell binding sites in domain VI of the laminin $\alpha 2$, $\alpha 3$, and $\alpha 5$ chains were identified by a systematic peptide screening. Four biologically active cell binding sequences from laminin $\alpha 2$ chain domain VI, two sequences from laminin $\alpha 3$ chain, and two sequences from the laminin $\alpha 5$ chain were identified. Five peptides promoted cell attachment activity in either the plate or bead assays and three peptides were active in the both assays. These results indicate that

We have sought to characterize the cellular receptors for the most active peptides. Cell attachment on A2-8 was inhibited by 5 mM EDTA, and five peptides showed reduced attachment in the presence of heparin. Previously, using this approach, we identified several cell binding sequences on the $\alpha 1$ chain, and three peptides, A13, AG10 and AG32, were found to recognize integrins (8, 10, 16). Cell attachment on A2-8 was cation-dependent, suggesting that this peptide has potential to interact with integrins, but this has not been tested. Recently, we found that the AG73 peptide interacted with syndecan-1 via its heparan sulfate side chains (15). Five peptides, whose cell attachment was inhibited by heparin, also likely interact with proteoglycans.

We aligned the domain VI sequences of the $\alpha 1$, $\alpha 2$, $\alpha 3$, and $\alpha 5$ chains (Figure 6). On the basis of the homologues observed, we focused on peptides A13, A2-7, and A5-16, which showed strong cell attachment activity and/or promotion of endothelial cell sprouting and tumor metastasis. In all of the α chains, the homologous sequences of A13 showed strong cell attachment activity in both peptide-coated plate assays (Table 3). A13 promoted cell adhesion, migration, angiogenesis, and tumor metastasis (10, 19, 24). A13 was also found to bind to integrin $\alpha 5\beta 1$ and $\alpha v\beta 3$ (16). Moreover, the homologous region of A13 on the laminin $\alpha 5$ chain was found to be active for cell binding by site-directed mutagenesis analysis of domain VI (35). These data

indicated that the results of active site mapping using synthetic peptides were comparable to that obtained using recombinant proteins. Taken together, the A13 region is an important site for biological activity.

A2–7 promoted cell attachment activity only in the plate assay, whereas the homologous peptides in the α 1, α 3, and α 5 chains did not show cell attachment activity. Furthermore, A2–7 was found to promote aortic sprouting in vitro and mouse lung colonization in vivo, whereas the homologous peptides did not show activity in these assays. These results suggest that the A2–7 sequence is specific in the laminin α 2 chain and has chain-specific biological activity.

A5–16 in the α 5 chain showed the strongest cell attachment activity in the plate assay. The homologous peptides in the α 2 and α 3 chains showed cell attachment activity, whereas α 1(A5–16) did not show activity, like A2–7. These results suggest that the A5–16 sequence also has chain-specific activity. These active peptides may be important for testing the cell-type specificity of the laminin α chains.

A13, A2–7, A2–8, and A3–10 promoted angiogenesis and tumor metastasis. We are not sure if these sites function in vivo in the intact molecule or in released fragments after matrix degradation. Various degradation products of extracellular matrix molecules can regulate tumor growth and angiogenesis. For example, a proteolytic fragment of laminin-5 (α 3 β 3 γ 2) generated by a matrix metalloproteinase was found to induce cell migration (36). Proteolytic fragments of plasminogen and collagen XVIII, designated angiostatin and endostatin, were also found to have important functions in regulating angiogenesis, tumor growth, and metastasis (37, 38). Proteolytic fragments of laminin chains may be involved in angiogenesis and tumor metastasis.

Using the synthetic peptide approach, a number of active sites on laminin-1 have been described. For example, some 20 active peptides have been described for endothelial cells (19, 20) while approximately 48 have been described for neuronal cells (42) on the laminin α 1, β 1, and γ 1 chains. Of the 20 peptides described for endothelial cells, four appear to be endothelial cell-specific (19, 20). Some peptides that are active with a variety of cells have different cellular responses dependent on the cell type. For example, AG73(RKRLQVQLSIRT, α 1 chain 2719–2730) promotes neurite outgrowth with neuronal cells (17), acinar formation with salivary gland cells (15), and metastasis with melanoma cells (18). The peptide approach is powerful for identifying active sites. The demonstration of specific cellular receptors for peptides adds support to their functional significance.

Here we describe the identification of cell binding sites in domain VI of the laminin α 2, α 3, and α 5 chains by systematic peptide screening. These active peptides suggest cell-type specificity of the laminin chains and thus, in part, define the reason for so many laminin isoforms.

REFERENCES

1. Colognato, H., and Yurchenco, P. D. (2000) *Dev. Dyn.* 218, 213–234.
2. Burgeson, R. E., Chiquet, M., Deutzmann, R., Ekblom, P., Engel, J., Kleinman, H. K., Martin, G. R., Meneguzzi, G., Paulson, M., Sanes, J., Timpl, R., Tryggvason, K., Yamada, Y., and Yurchenco, P. D. (1994) *Matrix Biol.* 14, 209–211.
3. Miner, J. H., Patton, B. L., Lentz, S. I., Gilbert, D. J., Snider, W. D., Jenkins, N. A., Copeland, N. G., and Sanes J. R. (1997) *J. Cell. Biol.* 137, 685–701.
4. Iivanainen, A., Morita, T., and Tryggvason, K. (1999) *J. Biol. Chem.* 274, 14107–14111.
5. Powell, S. K., and Kleinman, H. K. (1997) *Int. J. Biochem. Cell Biol.* 29, 401–414.
6. Yamada, Y., and Kleinman, H. K. (1992) 4, 819–823.
7. Yamada, K. M. (1991) *J. Biol. Chem.* 266, 12809–12912.
8. Nomizu, M., Kim, W. H., Yamamura, K., Utani, A., Song, S. Y., Otaka, A., Roller, P. P., Kleinman, H. K., and Yamada, Y. (1995) *J. Biol. Chem.* 270, 20583–20590.
9. Nomizu, M., Kuratomi, Y., Song, S. Y., Ponce L. M., Hoffman, M. P., Powell, S. K., Miyoshi, K., Otaka, A., Kleinman, H. K., and Yamada, Y. (1997) *J. Biol. Chem.* 272, 32198–32205.
10. Nomizu, M., Kuratomi, Y., Malinda, M. K., Song, S. Y., Miyoshi, K., Otaka, A., Powell, S. K., Hoffman, M. P., Kleinman, H. K., and Yamada, Y. (1998) *J. Biol. Chem.* 273, 32491–32499.
11. Nomizu, M., Kuratomi, Y., Ponce, L. M., Song, S.-Y., Miyoshi, K., Otaka, A., Powell, S. K., Hoffman, M. P., Kleinman, H. K., Yamada, Y. (2000) *Arch. Biochem. Biophys.* 378, 311–320.
12. Makino, M., Okazaki, I., Nishi, N., and Nomizu, M. (1999) *Connective Tissue* 31, 227–234.
13. Hoffman, M. P., Engbring, J. A., Nielsen, P. K., Vargas, J., Steinberg, Z., Karmand, A. J., Nomizu, M., Yamada, Y., and Kleinman, H. K. (2001) *J. Biol. Chem.* 276, 22077–22085.
14. Tashiro, K., Sephel, G. C., Grotrex, D., Sasaki, M., Shiraishi, N., Martin, G. R., Kleinman, H. K., and Yamada, Y. (1991) *J. Cell. Physiol.* 146, 451–459.
15. Hoffman, M. P., Nomizu, M., Roque, E., Lee, S., Jung, D. W., Yamada, Y., and Kleinman, H. K. (1998) *J. Biol. Chem.* 273, 28633–28641.
16. Ponce, M. L., Nomizu, M., and Kleinman, H. K. (2001) *FASEB J.* 15, 1389–1397.
17. Richard, B. L., Nomizu, M., Yamada, Y., and Kleinman, H. K. (1996) *Exp. Cell Res.* 228, 98–105.
18. Kim, W. H., Nomizu, M., Song, S. Y., Tanaka, K., Kuratomi, Y., Kleinman, H. K., and Yamada, Y. (1998) *Int. J. Cancer* 77, 632–639.
19. Malinda, M. K., Nomizu, M., Chung, M., Delgado, M., Kuratomi, Y., Yamada, Y., Kleinman, H. K., and Ponce L. M. (1999) *FASEB J.* 13, 53–62.
20. Ponce, M. L., Nomizu, M., Delgado, M. C., Kuratomi, Y., Hoffman, M. P., Powell, S., Yamada, Y., Kleinman, H. K., and Malinda, K. M. (1999) *Circ. Res.* 84, 688–694.
21. Colognato-Pyke, H., O'Rear, J. J., Yamada, Y., Carbonetto, S., Cheng, Y. S., and Yurchenco, P. D. (1995) *J. Biol. Chem.* 270, 9398–9406.
22. Colognato, H., MacCarrick, M., O'Rear, J. J., and Yurchenco, P. D. (1997) *J. Biol. Chem.* 272, 29330–29336.
23. Ettner, N., Gohring, W., Sasaki, T., Mann, K., and Timpl, R. (1998) *FEBS Lett.* 430, 217–221.
24. Kuratomi, Y., Nomizu, M., Nielsen, P., Tanaka, K., Song, S.-Y., Kleinman, H. K., and Yamada, Y. (1999) *Exp. Cell Res.* 249, 386–395.
25. Ehrig, K., Leivo, I., Argraves, W.S., Ruoslahti, E., and Engvall, E. (1990) *Proc. Natl. Acad. Sci. U.S.A.* 87, 3264–3268.
26. Rousselle, P., Lunstrum, G. P., Keene, D. R., Burgeson, R. E. (1991) *J. Cell Biol.* 114, 567–576.
27. Miner, J. H., and Li, C. (2000) *Dev. Biol.* 217, 278–289.
28. Ljubimov, A. V., Huang, Z. S., Huang, G. H., Burgeson, R. E., Gullberg, D., Miner, J. H., Ninomiya, Y., Sado, Y., Kenney, M. C. (1998) *J. Histochem. Cytochem.* 46, 1033–1041.
29. Lee, S. P., Cunningham, M. L., Hines, P. C., Jones, C. C., Orringer, E. P., Parise, L. V. (1998) *Blood* 92, 2951–2958.
30. Nomizu, M., Song, S. Y., Kuratomi, Y., Tanaka, M., Kim, W. H., Kleinman, H. K., and Yamada, Y. (1996) *FEBS Lett.* 396, 37–42.
31. Rasheed, S., Nelson-Rees, W. A., Toth, E. M., Arnstein, P., and Gardner, M. B. (1974) *Cancer* 33, 1027–1033.

32. Nicosia, R. F., and Ottinetti, A. (1990) *Dev. Biol.* 26, 119–128.
33. Yamamoto, S., Kaneda, Y., Okada, N., Nakagawa, S., Kubo, K., Inoue, S., Maeda, M., Yamashiro, Y., Kawasaki, K., and Mayumi, T. (1994) *Anti-Cancer Drugs* 5, 424–428.
34. Tashiro, K., Sephel, G. C., Weeks, B., Sasaki, M., Martin, G. R., Kleinman, H. K., and Yamada, Y. (1989) *J. Biol. Chem.* 264, 16174–16182.
35. Nielsen, P. K., and Yamada, Y. (2001) *J. Biol. Chem.* 276, 10906–10912.
36. Giannelli, G., Falk-Marzillier, J., Schiraldi, O., Stetler-Stevenson, W. G., and Quaranta, V. (1997) *Science* 277, 225–228.
37. O'Reilly, M. S., Holmgren, L., Shing, Y., Chen, C., Rosenthal, R. A., Moses, M., Lane, W. S., Cao, Y., Sage, E. H., and Folkman, J. (1994) *Cell* 21, 315–328.
38. O'Reilly, M. S., Boehm, T., Shing, Y., Fukai, N., Vasios, G., Lane, W. S., Flynn, E., Birkhead, J. R., Olsen, B. R., and Folkman, J. (1997) *Cell* 24, 277–285.
39. Bernier, S. M., Utani, A., Sugiyama, S., Doi, T., Polistina, C., and Yamada, Y. (1995) *Matrix Biol.* 14, 447–455.
40. Miner, J. H., Lewis, R. M., and Sanes, J. R. (1995) *J. Biol. Chem.* 270, 28523–28526.
41. Sasaki, M., Kleinman, H. K., Huber, H., Deutzmann, R., and Yamada, Y. (1988) *J. Biol. Chem.* 263, 16536–16544.
42. Powell, S. K., Rao, J., Roque, E., Nomizu, M., Kuratomi, Y., Yamada, Y., and Kleinman, H. K. (2000) *J. Neurosci. Res.* 61, 302–312.

BI011552C